The Meteoritical Society

Meteoritics & Planetary Science 49, Nr 3, 394–411 (2014)
doi: 10.1111/maps.12256

^{10}Be content in clasts from fallout suevitic breccia in drill cores from the Bosumtwi impact crater, Ghana: Clues to preimpact target distribution

Anna LOSIAK[1,2*], Eva Maria WILD[3], Leonard MICHLMAYR[3], and Christian KOEBERL[1,4]

[1]Department of Lithospheric Research, University of Vienna, Althanstrasse 14, A-1090 Vienna, Austria
[2]Institute of Geological Sciences, Polish Academy of Sciences, Podwale 75, 50-449 Wrocław, Poland
[3]VERA Laboratory, Faculty of Physics, Isotope Research and Nuclear Physics, University of Vienna, A-1090 Vienna, Austria
[4]Natural History Museum, Burgring 7, A-1010 Vienna, Austria
[*]Corresponding author. E-mail: anna.losiak@twarda.pan.pl

(Received 11 May 2013; revision accepted 25 November 2013)

Abstract–Rocks from drill cores LB-07A (crater fill) and LB-08A (central uplift) into the Bosumtwi impact crater, Ghana, were analyzed for the presence of the cosmogenic radionuclide ^{10}Be. The aim of the study was to determine the extent to which target rocks of various depths were mixed during the formation of the crater-filling breccia, and also to detect meteoric water infiltration within the impactite layer. ^{10}Be abundances above background were found in two (out of 24) samples from the LB-07A core, and in none of five samples from the LB-08A core. After excluding other possible explanations for an elevated ^{10}Be signal, we conclude that it is most probably due to a preimpact origin of those clasts from target rocks close to the surface. Our results suggest that in-crater breccias were well mixed during the impact cratering process. In addition, the lack of a ^{10}Be signal within the rocks located very close to the lake sediment–impactite boundary suggests that infiltration of meteoric water below the postimpact crater floor was limited. This may suggest that the infiltration of the meteoric water within the crater takes place not through the aerial pore-space, but rather through a localized system of fractures.

INTRODUCTION

During the impact cratering process, a large fraction of the surface layer of the target material is removed from the crater in the form of ejecta (mostly distal) or is vaporized/melted (e.g., Melosh 1989). Indeed, the formation of tektites from the uppermost layer of the target rocks has also been well established using the ^{10}Be contents of tektites (e.g., Pal et al. 1982; Ma et al. 2004; Serefiddin et al. 2007), as well as chemical comparison of tektites with their probable source-surface material (e.g., Koeberl 1994; Koeberl et al. 1997; Engelhardt et al. 2005; Son and Koeberl 2007), and reproduced by computer modeling (e.g., Artemieva 2000). However, some research suggests that near-surface target material may be incorporated in crater-filling breccias. This is based on studies of rare impact structures developed within target rocks characterized by easily distinguished, horizontal layers where the approximate depth of origin of clasts present in the resulting crater-filling suevite can be determined by their lithologic characterization. Two such craters are Kärdla, a 4 km wide, submarine, 455 Ma crater in Estonia (Puura et al. 2004) and Tswaing, a 1.13 km diameter, subaerial, 0.22 Ma crater in South Africa (Reimold et al. 1992). However, those studies are not sufficient to quantitatively evaluate the mixing process within the impact crater's transient cavity. Tswaing is a small crater, such that surface material can be easily incorporated into crater-filling breccias during the modification stage by slumping and similar mass-wasting processes (e.g., Melosh 1989). In addition, the exact percentage and location of the clasts originating near the surface that were incorporated in the crater-filling material of the Tswaing crater were not studied (Reimold et al. 1992), and the original drill core is not available for further studies (Reimold, personal communication). Drawing conclusions about the process of material mixing within the cratering event based on the Kärdla structure is even more problematic

(even though an excellent lithostratigraphic profile is available: Puura et al. 2004), because this crater was formed within a shallow <100 m deep sea (Puura et al. 2004). Multiple studies suggest that there are significant differences between subaerial and submarine craters with respect to the late stages of crater formation, including the process of mixing of the crater-filling material (e.g., Ormö and Lindstrom 2000; Ormö et al. 2010). To better understand the process of material mixing within the transient cavity of subaerial craters, more research is necessary.

Unfortunately, with respect to most subaerial craters, the approach used at Tswaing or Kärdla cannot be applied because target rocks are rarely horizontally stratified with layers easily distinguishable from each other. However, if the age of the impact crater is known and less than a few million years, the approximate depth of origin of clasts present within the suevitic breccia can be established using abundances of ^{10}Be within the clast.

^{10}Be is a cosmogenic radionuclide with a newly determined half-life of 1.386 ± 0.016 Ma (Chmeleff et al. 2010) or 1.388 ± 0.018 Ma (Korschinek et al. 2010), but other values are also in use: 1.36 ± 0.07 Ma (Nishiizumi et al. 2007) and 1.51 ± 0.06 Ma (Hofmann et al. 1987). It is produced in the atmosphere and in situ, primarily by spallation reactions, negative muon capture, or/and thermal neutron capture, due to the interaction of ^{16}O, ^{28}Si, and ^{9}Be with cosmic rays (Dunai 2010). As a result, the ^{10}Be content is enriched in the top few meters of surface materials (Pavich et al. 1985; Serefiddin et al. 2007; Dunai 2010; Graly et al. 2010), and could, therefore, be used to trace the surface origin of clasts displaced during the impact process. In addition, as ^{10}Be is enriched in meteoric water, this radionuclide can be used to trace water circulation within a drainage basin (e.g., Willenbring and von Blanckenburg 2010), such as an impact crater.

The Bosumtwi crater was chosen as an appropriate study site because of its relatively large size (10.5 km in diameter), relatively young age of 1.07 Ma (Koeberl et al. 1997), good preservation, and availability of samples from the drill core (Koeberl et al. 2007a). The size of 10.5 km minimizes the probability of incorporation of surface material by secondary processes (such as slumping) into the core during the modification stage of the crater formation process (e.g., Melosh 1989). The age of the crater of 1.07 Ma is comparable with the radionuclide half-life and thus young enough to allow the usage of the ^{10}Be system, so that it should be possible to recognize surface-derived material within available detection limits. Samples used in this study were obtained during the 2004 International Continental Scientific Drilling Program (ICDP) Lake Bosumtwi Drilling Project (e.g., Koeberl et al. 2007a). The sampled drill cores have previously been petrographically and geochemically described (e.g., Coney et al. 2007; Ferrière et al. 2007a, 2007b, 2008, 2010).

The aim of this study is to investigate if surface-derived, ^{10}Be-enriched (in situ and meteoric) material is present in the suevitic breccia of the Bosumtwi crater. This will help to determine the extent of mixing of target rocks during crater formation with respect to the fallback breccia. In addition, the topmost layer of the impactites was analyzed for elevated ^{10}Be contents, which may result from interaction with meteoric (lake) water after crater formation and could provide information about water circulation within a newly formed crater.

GEOLOGIC BACKGROUND

The Bosumtwi impact crater, located in Ghana, West Africa (Fig. 1) was formed at 1.07 Ma (e.g., Koeberl et al. 1997). It was excavated in rocks of the Early Proterozoic Birimian Supergroup of the West African craton (e.g., Jones et al. 1981). The Birimian Supergroup can be divided into two contemporary units (volcanic belts and sedimentary basins) aligned in multiple parallel structural features. In addition, numerous, extensive granitoid intrusions are present. The sedimentary unit of the Birimian Supergroup consists of volcaniclastic rocks, argillites, and turbidites that are now metamorphosed to meta-graywackes, phyllites, schists, and shales (Leube et al. 1990). The volcanic unit has a predominantly tholeiitic chemical composition and consists of metamorphosed basalts and andesites that occur as different types of schists, including hornblende-actinolite-, calcite-chlorite-, mica-schists, and in some cases amphibolites (Leube et al. 1990). The Birimian rocks were metamorphosed during the Eburnean tectono-thermal event at approximately 2092 Ma to greenschist and (locally) amphibolite facies (Feybesse et al. 2006).

The Bosumtwi impact crater was emplaced within a metasedimentary unit (mostly meta-graywackes, phyllites, and schists), close to the boundary with metavolcanics of the Ashanti belt (Fig. 1). In addition, in the proximity of the Bosumtwi crater, few small granitic bodies and dikes are present (e.g., Moon and Mason 1967; Jones 1985; Reimold et al. 1998; Koeberl and Reimold 2005; Losiak et al. 2013).

SAMPLES

Samples selected for this study come from the impactite layer of the LB-07A and LB-08A cores drilled within the Bosumtwi impact crater (Fig. 1) (e.g., Koeberl et al. 2007a). The detailed information on the

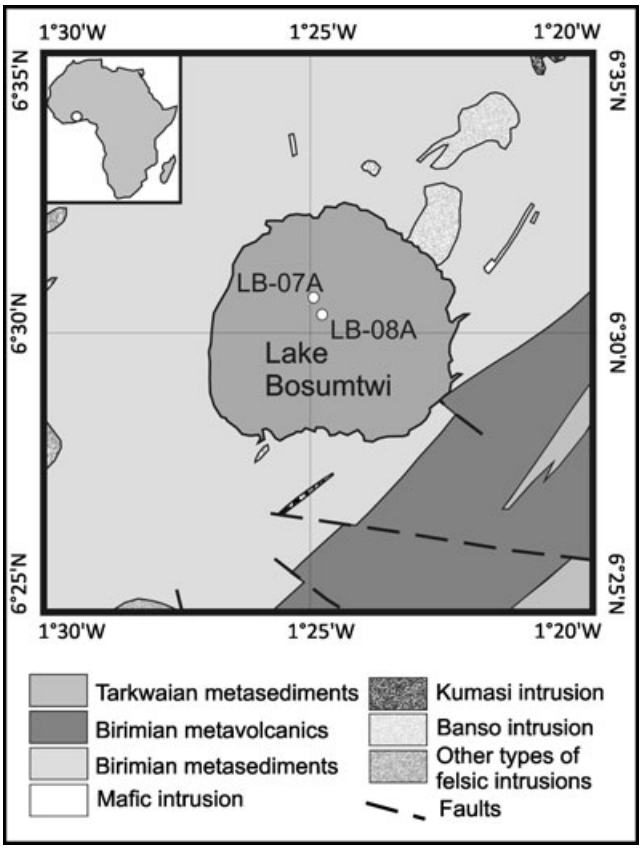

Fig. 1. Schematic geologic map of the Bosumtwi impact crater and location of drill cores LB-07A and LB-08A used in this study (adapted from Koeberl and Reimold [2005] and Losiak et al. [2013]).

lithostratigraphy, petrography, and geochemistry of those drill cores is available in Coney et al. (2007) and Ferrière et al. (2007a, 2007b) and is presented graphically in Fig. 2.

Core LB-07A was drilled in the deepest part of the impact crater and impactites come from depths between 333.38 and 545.08 m (Coney et al. 2007). It consists of three main sequences: (1) the upper impactites (333.38–415.67 m), composed of polymictic lithic breccias and suevite; (2) the lower impactites (415.67–470.55 m), composed of monomictic impact breccia with small suevite injections; and (3) shocked basement (470.55–545.08 m) (Coney et al. 2007).

Core LB-08A was drilled on the outer flank of the central uplift, with impactites having been recovered between 235.6 and 451.33 m depth within the drill core (Ferrière et al. 2007a). The top 25 m impactite sequence consists of polymict, clast-supported lithic breccia intercalated with suevite, while the other part of the core is a highly fractured, shocked metasediment, mostly meta-graywacke, phyllite, and slate (Ferrière et al. 2007a, 2007b).

In total, 29 samples were analyzed (Table 1): 16 single-clast samples selected from within breccia and 13 breccia samples (without clasts larger than approximately 1 cm^3 present). Twenty-four of them came from core LB-07A and represent depths of 333.7–407.9 m ("upper impactite layer"; Coney et al. 2007) and 5 are from core LB-08A from depths 239.5–264.9 m ("fallback breccia"; Ferrière et al. 2007a).

The process of single-clast sample selection was guided by the following objectives: (1) relatively uniform coverage of the entire drill core, (2) sampling only clasts larger than approximately 8 cm^3, (3) sampling clasts representing different lithologies present in the core. The breccia samples were selected (1) below the border between impactites and lake deposits to test for the possibility of ^{10}Be contamination by lake water infiltration, (2) if the core section appeared as if it could have been affected by hydrothermal processes (e.g., Karikari et al. 2007), (3) if there was no appropriate clast to be sampled within a significant segment from the core.

METHODS

Accelerator Mass Spectrometry

The ^{10}Be concentration in the environment is so low that the measurement can be performed only by accelerator mass spectrometry (AMS).

Sample Preparation for AMS

Sample preparation for the ^{10}Be AMS measurement consists of three stages: (1) dissolving samples, (2) separation of beryllium from the sample, and (3) preparing BeO AMS targets. The first stage was performed at the Department of Lithospheric Research, University of Vienna. At least 200 g of each sample was crushed with a hammer. To avoid contamination that could have been introduced during drilling, only pieces of sample that were inside the original clasts were selected for further analysis and pulverized in an agate mill. Powders were heated in a muffle furnace to 950 °C for 2 h to remove all organic compounds that could interfere with further steps of the sample preparation procedure (studies of ^{10}Be composition in tektites show that ^{10}Be is not affected by high temperature, e.g., Koeberl 1986, 1994; Wasson 2003; Serefiddin et al. 2007). Subsequently, samples were dissolved using an Anton Paar Multiwave 3000 microwave sample preparation system. This system consists of eight separate Teflon reactors; in each, there was approximately 0.1 g of rock powder added to a mixture of 22M HF, 15M HNO_3, and H_2O, as well as 0.6 mg or 1 mg of ^{9}Be carrier (see Table 1). After full

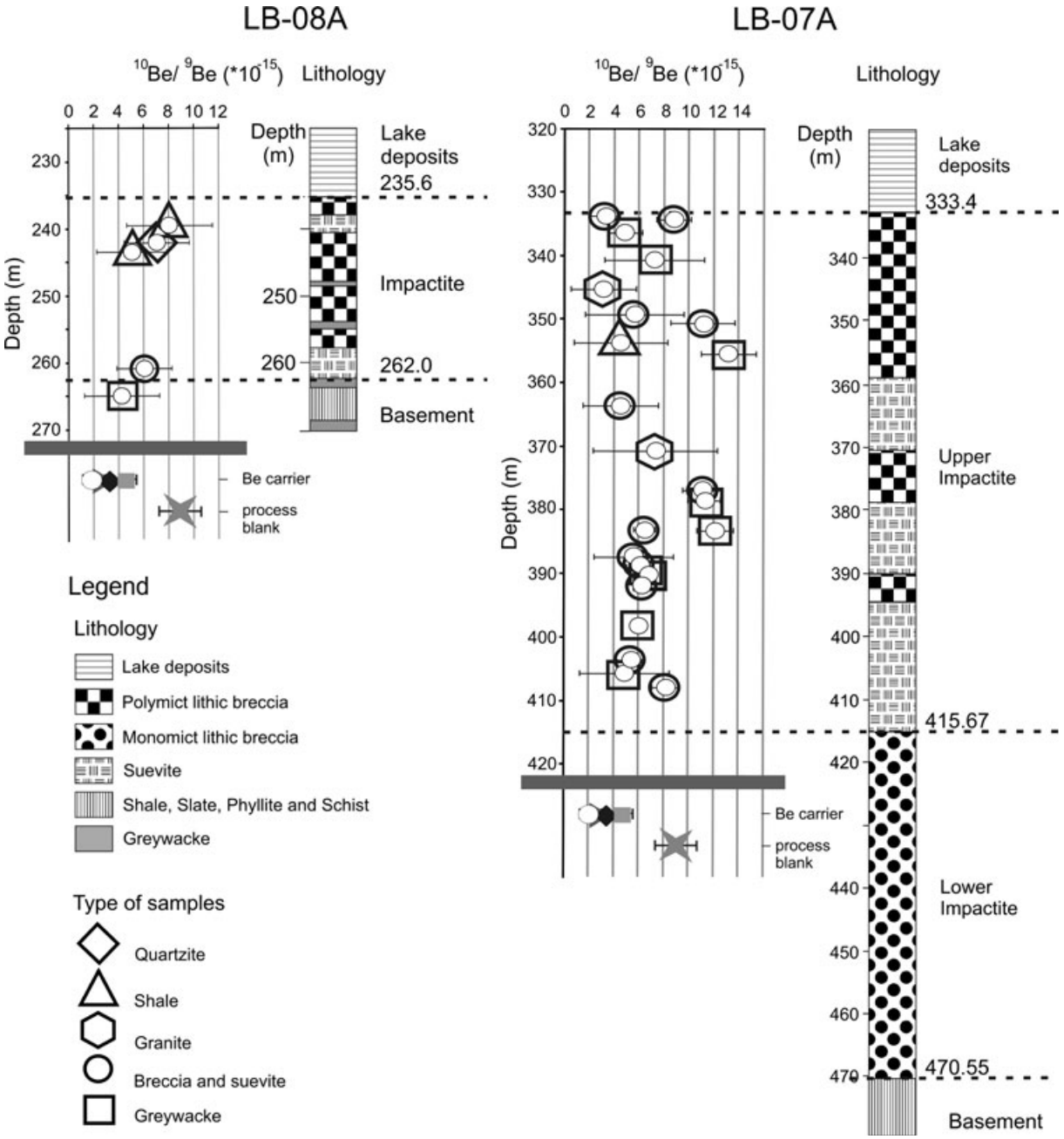

Fig. 2. ^{10}Be/^{9}Be ratios within samples studied in this project showed in a depth profile on a background of the lithologic information (data on drill core LB-07A from Coney et al. [2007] and on drill core LB-08A from Ferrière et al. [2007a]). The figure shows that there is no clear relationship between the depth of a sample and its measured ^{10}Be/^{9}Be ratio.

dissolution of the powders (usually after 4 h in 140 °C, but some samples required longer times to fully dissolve), samples were evaporated to dryness using the same sample preparation system. Subsequently, powders were redissolved in 7M HNO_3, evaporated to dryness, and then redissolved again in 6M HCl. After evaporating them to dryness for the third time, samples were dissolved in 6M HCl and all solutions belonging to the same sample were combined.

The second stage of sample preparation focused on chemical separation of beryllium from the dissolved sample. It was executed at the Vienna Environmental Research Accelerator Facility (VERA) at the Faculty of Physics, University of Vienna. The beryllium separation from the sample solution was performed by a combination of ion exchange operations (Korkisch 1989) and hydroxide precipitation steps. The chemical method used here is a slightly modified version of the

Table 1. Results of AMS measurements of ^{10}Be contents in the studied samples from the Bosumtwi crater.

Sample number	Drill core	Depth (m)	Sample type	Mass (g)	^{9}Be carrier (mg)	$^{10}Be/^{9}Be \times 10^{-15}$	$\pm(2\sigma) \times 10^{-15}$	Significance test ([a]) σ	$^{10}Be \times 10^{6}$ atom g^{-1}	$\pm(2\sigma) \times 10^{6}$ atom g^{-1}
AL1	8A	239.5	Shale	0.8045	1	8.1	3.4	−0.4	—	—
AL2	8A	243.4	Shale	0.8036	1	5.1	2.6	−2.4	—	—
AL3	8A	242.1	Quartzite	0.7118	1	7.1	2.8	−1.0	—	—
AL5	8A	260.9	Suevite	0.8061	1	6.1	2.2	−2.0	—	—
AL6	8A	264.9	Graywacke	0.8047	1	4.3	3.0	−2.6	—	—
AL7	7A	333.7	Breccia	0.8163	0.6	3.3	1.2	−5.4	—	—
AL8	7A	334.3	Suevite	0.8167	0.6	8.9	1.4	0.1	—	—
AL9	7A	336.4	Graywacke	0.8068	1	4.9	1.4	−3.6	—	—
AL11	7A	340.7	Graywacke	0.8075	1	7.3	4.0	−0.7	—	—
AL12	7A	345.2	Granite	0.8073	1	3.2	2.6	−3.6	—	—
AL13	7A	349.2	Breccia	0.8120	1	5.7	4.0	−1.4	—	—
AL14	7A	350.6	Suevite	0.8137	1	11.2	2.6	1.6	—	—
AL15	7A	353.7	Shale	0.8118	1	4.6	3.8	−2.0	—	—
AL18	7A	363.6	Suevite	0.8092	1	4.6	3.0	−2.5	—	—
AL21	7A	370.7	Granite	0.8147	1	7.4	5.0	−0.5	—	—
AL22	7A	377.0	Suevite	0.8152	0.6	11.2	1.6	2.1	—	—
AL24	7A	383.2	Suevite	0.8156	1	6.5	0.9	−2.5	—	—
AL25	7A	383.4	Graywacke	0.8172	1	12.2	1.5	3.1	0.28	0.12
AL26	7A	387.5	Breccia	0.8132	1	5.7	3.2	−1.7	—	—
AL28	7A	389.1	Graywacke	0.8175	0.6	6.1	1.0	−2.9	—	—
AL29	7A	390.1	Graywacke	0.8051	1	6.7	0.7	−2.4	—	—
AL30	7A	392.1	Suevite	0.8050	1	6.3	0.6	−2.9	—	—
AL33	7A	403.9	Suevite	0.8172	0.6	5.3	1.0	−3.7	—	—
AL37	7A	405.7	Graywacke	0.8141	1	4.9	3.6	−2.0	—	—
AL41a	7A	355.5	Graywacke	0.8051	1	10.7	0.7	2.1	—	—
AL41b			Graywacke	0.8236	0.6	13.3	2.2	3.3	0.33	0.11
AL42	7A	385.2	Suevite	0.8207	0.6	8.9	1.1	0.2	—	—
AL43	7A	398.3	Graywacke	0.7027	1	6.0	0.5	−3.3	—	—
AL44	7A	407.9	Suevite	0.8112	0.6	8.2	1.1	−0.6	—	—
AL45	7A	378.6	Graywacke	0.8179	0.6	11.3	1.3	2.4	—	—

Measurements were performed during four independent sessions: A (AL29, AL30, AL41, AL43), B (AL03, AL05, AL06, AL09, AL11), C (AL01, AL02, AL12, AL13, AL15, AL18, AL21, AL26, AL37), D (AL07, AL08, AL14, AL18, AL22, AL24, AL25, AL28, AL33, AL41, AL42, AL44, AL45).

The transmission from the high energy currents to the detector signal is between 30.63% for A session, 25.53% for B session, 5.83% for C session, and 27.72% for D session. The precision of the calibration is 0.19% for the A session, 2.5% for the B session, 2.76% for the C session, 1.06% for the D session. This is a correlated uncertainty included in the uncertainties listed in the table. The uncertainty of the standard definition is not considered. The isotope ratios are normalized to the standard. No background correction has been applied.

$^{10}Be/^{9}Be$ ratio of the beryllium carrier was measured four times: A: $(2.78 \pm 0.34) \times 10^{-15}$, B: $(2.52 \pm 0.96) \times 10^{-15}$, C: $(3.79 \pm 1.9) \times 10^{-15}$, and D: $(1.64 \pm 0.52) \times 10^{-15}$.

$^{10}Be/^{9}Be$ ratio of the process blank was measured to be $(8.79 \pm 1.62) \times 10^{-15}$.

^{10}Be in at/g values are blank-corrected, but not decay-corrected.

[a]Significance test—checks if the sample is significantly different than the process blank by calculating confidence interval for difference between population means. Samples characterized by the calculated values >3 are significantly different from the process blank with a 99.73% probability.

method described by Auer (2007) and Auer et al. (2007).

At first, the samples previously dissolved in 6M HCl were passed through the anion exchange column (filled with resin Biorad AG1-X8 100-200 mesh) to remove iron. Then beryllium and aluminum hydroxides were precipitated at pH of 8 with NH_3 (aq) to remove Ca and Ni (Merchel and Herpers 1999) as well as to decrease the size of the solution produced afterward. Hydroxide samples were redissolved in few milliliters of 0.5M HCl and passed through the cation exchange column (filled with resin Biorad AG50W-X8 100-200 mesh) to separate beryllium from aluminum. In this step, beryllium is also largely separated from boron. In most cases, due to a very high amount of aluminum present in the samples (from 25 to 113 mg), this step of the chemical separation had to be performed twice (with the precipitation in between).

To determine beryllium yields of the sample preparation method, aliquots of the sample solutions were taken after every step of the chemical procedure and the Be and Al contents were measured with atomic absorption spectroscopy. The total beryllium yields of the chemical separation method were determined to be approximately 80%.

In the third stage, the AMS targets were produced by precipitating Be as hydroxide, which was then converted to oxide by heating and afterward pressed into targets. At first, beryllium hydroxide was precipitated and washed three times with double distilled water to remove boron, which interferes with the AMS ^{10}Be measurement. Then the precipitate was transferred into small quartz crucibles, and heated for 4 h at 850 °C to dehydrate the $Be(OH)_2$ to BeO. BeO was mixed with small amount of Cu powder and pressed into copper AMS targets. As beryllium is highly toxic, all steps of the AMS target preparation were done in a fume hood or in a glove box.

Carrier and Standards for AMS Measurements

The ^{9}Be carrier that was used in this study was a beryllium standard by Merck for conventional mass spectrometry (MERC 19775 41466612). The amount of the carrier added varied between 0.6 and 1 mg of beryllium (Table 1). Its ^{10}Be/^{9}Be ratios scattered between $(1.64 \pm 0.52) \times 10^{-15}$ and $(3.79 \pm 1.9) \times 10^{-15}$ (2σ uncertainty) and on average was 2.7×10^{-15}. The measured ^{10}Be/^{9}Be ratio of a process blank was $(8.79 \pm 1.6) \times 10^{-15}$ (Table 1).

The ^{10}Be/^{9}Be ratio of the process blank is somewhat higher than the average ratio of the carrier. However, 15 of the measured samples have ^{10}Be/^{9}Be ratios that are indistinguishable (within 2σ uncertainty) from values characteristic from the highest measured ratio of beryllium carrier used in this study $(3.79 \pm 1.9) \times 10^{-15}$, and are significantly lower than in the process blank (Table 1). This shows that the real ^{10}Be/^{9}Be ratio of the process blank is in most cases lower than $(8.79 \pm 1.62) \times 10^{-15}$.

The ^{10}Be standard used in this study is the NIST SRM4325 (NIST = National Institute of Standards and Technology) with certified ^{10}Be/^{9}Be ratio of 2.68×10^{-11} ($\pm 5.1\%$); however, according to Nishiizumi et al. (2007), a more precise value of this standard is $(2.79 \pm 0.03) \times 10^{-11}$. Our results are referenced to the NIST value.

Measurement by AMS

^{10}Be/^{9}Be ratios were measured with the VERA AMS system (see e.g., Kutschera et al. 1997; Steier et al. 2004)—using a post-stripping method for isobar separation (e.g., Michlmayr 2007). The method addresses the discrimination between ^{10}Be and its isobar ^{10}B by using the difference in energy loss of the ion beam in matter, due to the different atomic number of ^{10}Be and ^{10}B (Michlmayr 2007). The VERA AMS machine background for ^{10}Be varies between 8×10^{-16} and 3×10^{-15} (Michlmayr 2007). Detailed information on the setup and performance of the VERA during the ^{10}Be measurement was described in Martschini (2008).

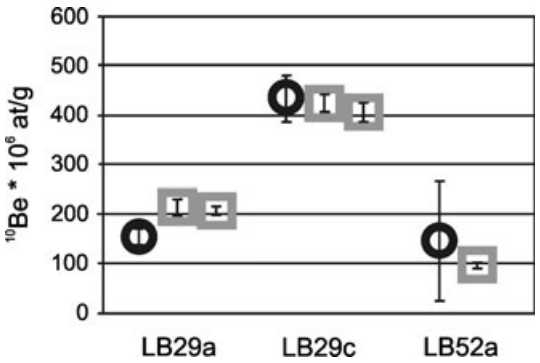

Fig. 3. Comparison of results obtained by Serefiddin et al. (2007) (black circles) and in this study (gray squares) on soil samples from the Bosumtwi region with the 2σ errors plotted. The plot shows a generally good agreement with previously published data (within error).

Results of the Pilot Project

To develop an efficient method of sample preparation, as well as assess the accuracy and reproducibility of the measurement and sample preparation method, a pilot project was performed on soil samples from the Bosumtwi region previously measured by Serefiddin et al. (2007). Our results show a generally good agreement with previously published data (within uncertainty) (Fig. 3). However, results obtained for sample LB29a are somewhat higher than those measured by Serefiddin et al. (2007). To test the precision of our method, we have processed samples LB29a and LB29c twice (Fig. 3). Two subsamples of the sample LB29a were processed separately throughout the entire procedure to test reproducibility and precision of the sample preparation process. Sample LB29c was divided into two separate targets at the very end of the procedure to test reproducibility and precision of AMS measurement. The results of the pilot project show good accuracy and precision for both sample preparation and the AMS measurement applied in this study.

RESULTS

The detailed petrographic characteristics of the samples are provided in Table 2. The studied samples can be divided into a few petrologic groups. Out of a

Table 2. Petrologic description of samples (specific clasts that were dissolved for ^{10}Be analysis) from the Bosumtwi impact crater (cores LB-07A and LB-08A) analyzed in this study.

Sample number	Drill hole	Depth (m)	Sample description	Shock metamorphic properties
AL1	8A	239.5	Highly altered graphitic shale. The fine-grained matrix is composed of quartz, feldspar, micas (sericite and chlorite), graphite, and some accessory minerals, including titanite, epidote, and rutile as well as some opaques. Few cross-cutting sets of quartz veinlets are present.	PDFs are present in the quartz veinlets (up to three cross-cutting sets). In addition, some of the quartz grains display a "toasted appearance."
AL2	8A	243.4	Well-banded graphitic shale (or phyllite), with a mylonitic quartz ribbons. Some of the bands consist of large quartz grains. Large subhedral grains of graphite are present.	Rare and faint PDFs are present in some of the quartz grains.
AL3	8A	242.1	Quartzite consisting mostly of very large quartz grains, with some areas where much smaller grain size is prevailing.	Most of the grains in the sample include some PDFs. Some of the enclaves additionally appear to be "toasted."
AL5	8A	260.9	Suevite consisting mostly of fine-grained graywacke-derived matrix (quartz, feldspar, and micas), and clasts of graywacke and well banded graphitic shale. Melt clasts are scare.	Some quartz grains are highly shocked and toasted (but most are too small to see indications of shock metamorphism).
AL6	8A	264.9	Fine-grained, mylonitized graywacke composed of mostly quartz, feldspar, and various micas (sericite and chlorite). Sample is highly altered, with abundant occurrences of amorphous reddish phase.	Some quartz grains contain PDFs.
AL7	7A	333.7	Monomictic breccia composed of fine-grained, mylonitized graywacke with large clasts present. The fine-grained matrix is composed of quartz, feldspar, and micas (mostly sericite and chlorite).	Rare and faint PDFs are present in some of the quartz grains.
AL8	7A	334.3	Matrix-rich suevite consisting of large variety of lithic and mineral clasts: fine- and medium-grained meta-graywacke, slate, phyllite, quartzite, as well as few melt clasts (brown and subrounded). Sample similar to samples AL18 and AL41.	Some clasts (or fragments of grains) are isotropized, probably due to heating. No grains bearing PDFs were identified.
AL9	7A	336.4	Fine-grained, mylonitized graywacke composed of mostly quartz, feldspar, and various micas (sericite and chlorite) showing a number of rotated and recrystallized quartz porphyroclasts. Sample is highly altered.	Rare and faint PDFs are present in some of the quartz grains.
AL11	7A	340.7	Medium-grained, partially mylonitized graywacke composed of matrix of quartz, feldspar, and various micas (sericite and chlorite) and quartz porphyroclasts. Sample is highly altered (although some not fully sericized feldspars are present).	Faint PDFs are present in multiple quartz grains.
AL12	7A	345.2	Medium-grained granite consisting of numerous quartz grains, feldspars (mostly twinned K-feldspar) in large part turned to sericite, and micas (mostly chlorite and sericite), as well as accessory rutile tourmaline and unidentified anhedral opaques. Sample is highly altered.	PDFs are common in the quartz grains present in this sample.
AL13	7A	349.2	It was impossible to prepare a thin section because the sample was not lithified.	
AL14	7A	350.6	Suevite consisting mostly of crushed clasts (that partially conserve the previous texture) of fine- and medium-grained meta-graywacke and phyllite. Few melt particles (brown subrounded) are also present.	Quartz grains rarely display PDFs.

Table 2. *Continued*. Petrologic description of samples (specific clasts that were dissolved for ^{10}Be analysis) from the Bosumtwi impact crater (cores LB-07A and LB-08A) analyzed in this study.

Sample number	Drill hole	Depth (m)	Sample description	Shock metamorphic properties
AL15	7A	353.7	Very fine-grained, slightly mylonized shale, with few narrow, somewhat darker bands (possibly due to higher contents of graphite).	No shock metamorphic effects were observed.
AL18	7A	363.6	Similar to sample AL08 and AL41.	Shock metamorphic effects are especially common within grains embedded within matrix.
AL21	7A	370.7	Medium-grained granite consisting of numerous quartz grains, feldspars (mostly twinned K-feldspar) in large part turned to sericite, and micas (mostly chlorite and sericite), as well as accessory rutile turmaline and unidentified anhedral opaques. Sample is in the early stage of mylonitization (some of the sericite and chlorite is oriented) and elongated opaque-rich pockets are present.	Up to two sets of PDFs in a grain were observed.
AL22	7A	377	Melt-rich suevite without any lithic clasts. Matrix is composed mostly of melt particles of various sizes (from few tens mm to few um) and of clasts of single grains. Significant amount of calcite is present.	Some grains do not display any signs of shock metamorphism, while others are highly shocked (especially ones being single clasts embedded within matrix).
AL24	7A	383.2	Suevite with a large variety of lithic and mineral clasts, including meta-graywacke, slate, phyllite, and quartz and feldspar grain clasts within very fine-grained matrix. Some of the lithic clasts are fully or partially isotropized (probably due to heating during the impact event), and often they have rounded outline.	Up to two sets of PDFs in a grain were observed.
AL25	7A	383.4	Highly shock-heated medium-grained, mylonitized graywacke with locally significant amount of opaques (possibly graphite) present.	Some grains contain very short PDFs.
AL26	7A	387.5	Monomictic breccia composed of fine-grained, mylonitized graywacke with large clasts present. The fine-grained matrix is composed of quartz, feldspar, and micas (mostly sericite and chlorite).	Grains are too small to observe PDFs. Some of the clasts or fragments of clasts are isotropized.
AL28	7A	389.1	Coarse-grained, partially mylonitized graywacke composed of matrix of quartz, feldspar, and various micas (sericite and chlorite), as well as quartz and feldspar porphyroclasts. Sample is highly altered (although some not fully sericized feldspars are present). Highly altered, alteration phases were probably heated during the impact event, and now are in a form of amorphous or microcrystalline material. Very similar to sample AL 30.	Small, short PDFs are observed in some grains.
AL29	7A	390.1	Very fine-grained, not mylonized graywacke with high amount of graphite present.	No shock effects are observed (possibly due to the very small size of the grains).
AL30	7A	392.1	Very similar to sample AL 28.	Faint, short PDFs are observed.
AL33	7A	403.9	Fine-grained suevite with small dispersed melt clasts and few small lithic clasts (of banned phyllite), most clasts are mineral (quartz and feldspar).	PDFs were not observed.

Table 2. *Continued*. Petrologic description of samples (specific clasts that were dissolved for ^{10}Be analysis) from the Bosumtwi impact crater (cores LB-07A and LB-08A) analyzed in this study.

Sample number	Drill hole	Depth (m)	Sample description	Shock metamorphic properties
AL37	7A	405.7	Slightly mylonitized medium-grained graywacke composed of matrix of quartz feldspar and various micas (sericite and chlorite) as well as quartz and feldspar porphyroclasts. Sample is relatively altered and includes significant amount of opaque material (probably graphite).	Some grains have short and relatively faint PDFs present.
AL41	7A	355.5	Medium- to coarse-grained slightly mylonitized meta-graywacke dominated by large quartz and feldspar clasts in a fine-grained matrix of phyllosilicates, quartz, feldspars, and opaques (possibly graphite). Similar to sample AL 45.	Large fraction of the quartz grains include PDFs.
AL42	7A	385.2	Very similar to sample AL 22.	Rare and faint PDFs are present.
AL43	7A	398.3	Strongly mylonitized medium-grained graphitic graywacke. It is composed of: large recrystallized quartz and feldspar clasts in a fine-grained matrix of mostly phyllosilicates (oriented), but also quartz, feldspars, and opaques.	No PDFs (or other signs of shock metamorphism) are observed.
AL44	7A	407.9	Sample similar to AL 08 and AL 18.	Some quartz grains present in the matrix include PDFs.
AL45	7A	378.6	Similar to sample AL 41, but more porous and more highly damaged by shock.	Rare grains include PDFs.

PDFs = planar deformation features—features developed in minerals, especially notable in quartz, as a response to shock metamorphism, K-feldspar = potassium feldspar $KAlSi_3O_8$.

total of 16 clasts, 2 were identified as granite, 10 as graywacke (or meta-graywacke), 3 as shales, and 1 clast as quartzite. Thirteen samples are impact breccias, and ten of them include melt clasts (and were classified as suevite). Most of the samples are shocked to some extent; quartz grains have up to three planar deformation feature (PDF) sets, some of them also having a "toasted" appearance (Ferrière et al. 2009).

The ^{10}Be/^{9}Be ratios have been measured during four independent AMS sessions (Table 1; Fig. 4). The transmission from the high-energy currents to the detector signal was about 30% for sessions A, B, and D. For session C, the transmission was much lower and only about 6% due to problems related to terminal voltage instability that resulted in much lower count rates and higher errors. The results of the AMS measurements are presented in Table 1 and Fig. 4.

All measured ^{10}Be/^{9}Be ratios are very close to the values characteristic for the ^{10}Be machine background as well as process blank used in this study; however, several different observations point to the conclusion that process blank (measured during the last session) represents the highest range of ^{10}Be introduction during sample preparation. First, all 18 samples (except one: AL41) measured during the first three sessions (A, B, and C) have their ^{10}Be/^{9}Be ratios indistinguishable within 3σ from the long-term measured machine blanks. This suggests that during the first three sessions, no significant amount of ^{10}Be was introduced during the sample preparation. Measured elevated value of AL41 is clearly different than any other sample measured during the first three sessions. It is true, however, that a few samples (e.g., AL44, AL8, and AL42) measured during session D show some signs of ^{10}Be being brought in during sample preparation and their ^{10}Be/^{9}Be ratio is consistent with the ratio of measured process blank. At the same time, some of the samples prepared and measured during session D are among the lowest values measured (e.g., AL07 and AL33).

Second, all but six samples form a uniformly increasing array on a plot presenting all samples arranged by their ^{10}Be/^{9}Be ratio, with measured process blank corresponding to the highest measured sample within this array. However, six samples with ^{10}Be/^{9}Be ratio above the measured process blank are characterized by values significantly (on 2σ level, except sample AL14 that has especially high error) higher than the highest sample from the array (Table 1). This suggests that those six measured samples (five unique and one duplicate of sample AL41) have an internal ^{10}Be that is not related to a sample contamination during chemical processing. We expect that remeasuring samples AL14, AL22, and AL45 (prepared with a higher amount of sample dissolved and a lower amount of beryllium carrier) might yield results

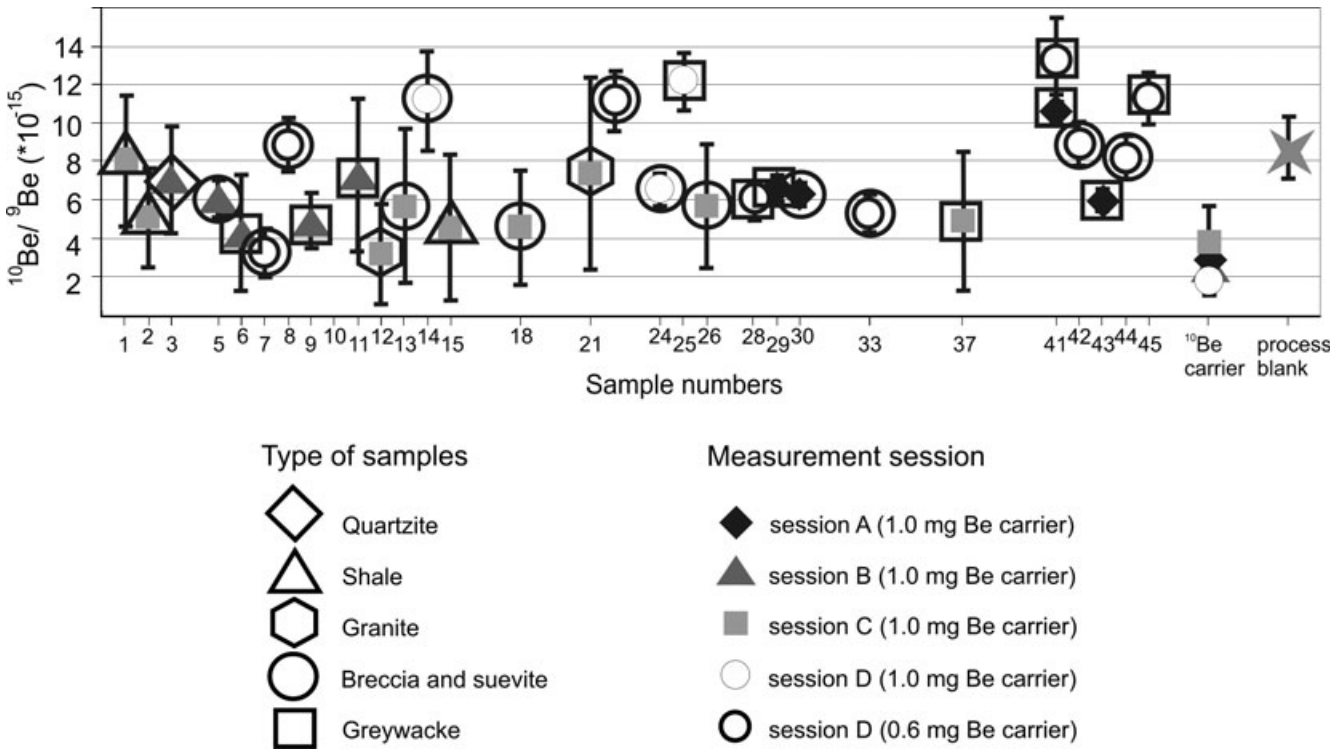

Fig. 4. ^{10}Be/^{9}Be ratios measured in samples from the Bosumtwi crater (error bars plotted as 2σ). Numbers on the horizontal axis correspond to the sample number (see Table 1).

that are different from the measured process blank on 3σ significance level. However, with samples measured within the scope of this study, only two (AL25 and AL41) were significantly different from the process blank (on 3σ level).

Third, sample AL41 was measured twice. The first measurement: $(10.7 \pm 0.7) \times 10^{-15}$ was performed during the session A, where all other samples were within level of a long-term machine blank. The second measurement $(13.3 \pm 2.2) \times 10^{-15}$ during the session D was performed with smaller amount of beryllium carrier. Both measurements were the same within 2σ error, but as expected, the measurement with lower amount of beryllium carrier yielded a higher ^{10}Be/^{9}Be ratio. The measurement consistency and following expected trend show that it is highly improbable that sample AL41 does not have some internal ^{10}Be.

Fourth, variation within the AMS does not explain the obtained results, especially higher scattering of the ^{10}Be/^{9}Be ratios measured during the D session. However, this seems to be related to (1) excess ^{10}Be present in the samples, and (2) small ^{10}Be introduction during the chemical sample preparation (as discussed above). There is no correlation between measured ^{10}Be/^{9}Be ratios and $^{9}Be^{2+}$ beam current or boron count rates. In addition, the in-house standards measured during every session were consistent with expected values of approximately 3×10^{-12} and 3×10^{-13} (based on long time measurements) and stable during the entire session.

Finally, sample AL41 was measured twice and both measurements were performed with the same amount of sample, but with different amounts of beryllium carrier: 1 and 0.6 mg, yielding ^{10}Be/^{9}Be ratios of $(10.7 \pm 0.7) \times 10^{-15}$ and $(13.3 \pm 2.2) \times 10^{-15}$, respectively. As expected, if the ^{10}Be is derived from the sample, the second measurement with the lower amount of carrier used resulted in a higher ^{10}Be/^{9}Be ratio.

Combining the five reasons mentioned above, we think that in the case of the two samples (AL25 and AL41) we can successfully confirm detection of excess ^{10}Be in the clasts and exclude random variations in the measured ^{10}Be/^{9}Be ratios due to machine performance and chemical preparation as a source of the signal. However, it is true that, because of very small amount of ^{10}Be present and lack of more precise estimation on the exact ratio of the full process blank, the calculated contents of the ^{10}Be within clasts are provided with a relatively large error. This limits our ability to estimate the exact depth of the clast origin within the preimpact target rocks.

As mentioned above, two samples (AL25, AL41) have ^{10}Be/^{9}Be ratios significantly (>3σ) above the process blank based on the confidence interval for the

difference between population means (e.g., Franklin 2007). In addition, their 2σ confidence intervals do not overlap with the process blank 2σ confidence interval. Only those two samples are discussed in this study as ones having a true ^{10}Be signal. Because of that, the numbers of ^{10}Be atoms per gram of sample were calculated only for those samples (Table 1). The sample AL25 is a graywacke clast collected on the depth of 383.2 m of the core LB-07A, and the sample AL41 is also a graywacke clast collected from depth of 355.5 m within the same core.

Two additional samples (AL22, AL45) have ^{10}Be/^{9}Be ratios higher than the process blank on more than 2σ (but less than 3σ) confidence level. We acknowledge that those samples probably include some internal ^{10}Be. But the experimental setup used in this study was not sufficient to confirm that those samples contain ^{10}Be with a 3σ probability level. 3σ threshold instead of more commonly used 2σ level is used in this study because we are basing our process blank estimate on a single measurement. Samples AL22, AL45, and AL14 will not be discussed in detail in the following section of the manuscript as ones with a detected ^{10}Be signal.

DISCUSSION

Possible Explanations of the Obtained Data

There are multiple explanations for the measured ^{10}Be/^{9}Be ratios of the samples above the blank value (1) laboratory contamination, (2) contamination introduced during drilling, (3) introduction of the ^{10}Be by meteoric water after crater formation, and (4) surface exposure of the clasts prior to the Bosumtwi crater formation. In the following section of the paper, we will discuss and evaluate their validity in explaining our data.

Laboratory Contamination

If isotopic values measured are as close to the blank value as ones in this study, it is especially easy to introduce contamination during the sample processing in the laboratory. However, explaining the increased ^{10}Be/^{9}Be ratios in samples AL25 and AL41 by laboratory contamination seems to be very unlikely. First, the samples with high ratios were processed in different groups, excluding a single source of contamination (e.g., a contaminated reactant or an error during the sample preparation). In addition, samples with the highest (e.g., AL41) and lowest (e.g., AL07) ^{10}Be/^{9}Be ratios were processed and measured together. Second, as no foreign samples with high ^{10}Be/^{9}Be ratios were processed together with our samples (except standards that were prepared separately), there is no obvious source of possible contamination. And finally, one of the samples with elevated ^{10}Be/^{9}Be ratio (AL41) was processed twice, each time giving the same (within 2σ) result. More importantly, the second measurement (AL41b), with a lower amount of ^{9}Be carrier, gave a higher ^{10}Be signal than during the first measurement (AL41a) with higher amount of carrier, confirming that the increased ^{10}Be signal comes from the sample, not from the carrier. All of those observations show that sample preparation method failure is an unlikely explanation of the obtained data.

Sample Contamination during Drill Cores Recovery

As mentioned before, ^{10}Be is mostly produced by the spallation of oxygen and nitrogen in the atmosphere at the rate dependent on the altitude, latitude, variations of the strength of magnetic field with time (Dunai 2010), at present on average amounting to approximately 1×10^6 at cm^{-2} yr^{-1} (Gosse and Phillips 2001). Because of that, its concentration is high in rain water and can vary between 1×10^3 at/g up to even approximately 1×10^5 at/g (Brown et al. 1992; Graham et al. 2003; Heikkilä et al. 2008; Willenbring and von Blanckenburg 2010), and in surface waters can be up to 3200 at/g (Brown et al. 1992; Willenbring and von Blanckenburg 2010). However, the ^{10}Be concentration in most surface waters is much lower and strongly dependent on many variables, such as the chemical properties and history of the water. In most terrestrial surface conditions, beryllium has a tendency to strongly adhere to soil grains: the partition coefficient is approximately 10^5 mL g^{-1} at pH >6 (but is much less in acidic conditions) (You et al. 1989). Some ^{10}Be can be also incorporated into clays, organic matter, or oxyhydroxides (e.g., Barg et al. 1997).

As a combined ^{10}Be signal from the in situ and meteoric ^{10}Be was measured in this study, contamination of the samples might have also occurred during drilling (from the lake water) or initial sample storage in Ghana (from rain water falling on the samples). If this is true, we could expect that entire sections of the core (or rather entire boxes with samples) should be affected by ^{10}Be contamination in a similar way. However, this is not the case in our data set. Samples characterized by the highest ^{10}Be/^{9}Be ratios are often located very close in the drill core to samples with very low or average ^{10}Be/^{9}Be ratio. For example, sample AL41, having the highest ratio measured in this study, is located only 1.8 m from sample AL15 with one of the lowest measured ratios. Both samples were stored in the same sample box. Even more extreme is the example of sample AL25 with ^{10}Be/^{9}Be ratio of $(12.2 \pm 1.5) \times 10^{-15}$, while sample AL24, located only 0.2 m from sample AL25, has ^{10}Be/^{9}Be ratio of

$(6.5 \pm 0.9) \times 10^{-15}$. In addition, the breccias should be much more affected by this process (due to much more surface area allowing beryllium to adhere to the grains) than clasts. However, this is not the case in our data set (Table 1; Fig. 4).

Introducing ^{10}Be by Interaction with Surface Water

^{10}Be present in the measured samples could also come from the meteoric water that might have infiltrated the fallback impactite layer soon after the crater was formed. The Bosumtwi crater is currently located within a humid climate zone, where the average annual rainfall varies from 1380 to 1550 mm yr^{-1} (Turner et al. 1996). Detailed research of the paleoclimate at this site shows that the Bosumtwi area was most probably relatively wet for most of its history (e.g., Shanahan et al. 2012), suggesting that the crater should have been filled with water soon after its formation. As Bosumtwi is a closed basin with limited amount of the groundwater inflow into the lake, most of the water-balance models suggest that the main source of water within Bosumtwi Lake is rainfall (e.g., Turner et al. 1996).

To test the meteoric-derived lake water contamination hypothesis, three samples collected close to the lake sediment–impactite contact within drill core LB-08A were analyzed. They came from depths of 239.5 m, 242.1 m, and 243.4 m blf, respectively, while the sediment–impactite contact was at an estimated depth of 235.6 m. It was impossible to collect samples closer to the contact because that part of the core was not available. Results show (Fig. 2) that, even though there seems to be a slight decrease of the detected ^{10}Be signal with increasing depth below the contact, all obtained results are the same within the 2σ error (and even 1σ error). In addition, all measured values are within the ^{10}Be/^{9}Be ratio of the process blanks used in this study.

Even more importantly, the measurement of sample AL07 from the drill core LB-07A argues against the hypothesis of contamination introduced by interaction with surface waters. This sample is collected from a depth of 333.7 m, just 0.3 m below the lake sediment–impactite contact, so if contamination occurred, it should have been heavily affected. In addition, sample AL07 is a monomictic breccia, characterized by a high surface area, prone to adsorbing ^{10}Be on the surface of grains within this sample (You et al. 1989; Shen et al. 2004; Graly et al. 2010). This suggests that if fluids with elevated ^{10}Be contents reached this depth, it is reasonable to expect that sample AL07 would have an elevated ^{10}Be/^{9}Be ratio.

Lack of the ^{10}Be signal only 0.3 m from the lake sediment–impactite contact could be potentially explained by the hypothesis that the top 0.3 m of impactite layer was extremely efficient in adsorption of the ^{10}Be, so that none of this element managed to reach depth of 0.3 m. However, the measured depth profiles of ^{10}Be within soil and regolith (e.g., Graly et al. [2010] and references within) argue against this explanation. The second possibility is that the impactite layer was separated efficiently from the surface water influence. Initially, the separation could have been provided by the fallback layer: an approximately 30 cm thick layer consisting of "accretionary lapilli, microtektite-like glass spherules, and shocked quartz grains" retrieved from LB-05 core drilled within the Bosumtwi impact structure (Koeberl et al. 2007b). A similar layer was probably present on the entire crater floor, apparently creating an efficient barrier between lake and impactite deposits. Later on, this separation could have been increased by the thick layer of lake sediments being deposited.

The lack of a significant amount of percolation into the topmost layer of impactites does not mean that there was no contact between surface water and impact-affected rocks. In fact, Karikari et al. (2007) as well as Petersen et al. (2007) found evidence supporting the existence of a hydrothermal system within Bosumtwi crater. Surface water could have penetrated the impactite layer through cracks within the fallback layer: if cracks were large enough to limit the particle–water interaction (and/or chemical properties of water allowed for beryllium to stay in solution), then some amount of ^{10}Be could have been prevented from adhering on the surface of grains located at low depth and transferred down the impactite section. In this case, we could expect an increased ^{10}Be signal along the fractures, and that breccias or suevites would be more affected than clasts (due to their higher surface area). However, the ^{10}Be/^{9}Be ratio measured in samples AL24 and AL25 located only 0.2 m from each other does not support this hypothesis, because sample AL24 is a suevite (with a high surface area allowing for preferential ^{10}Be adsorption), which is characterized by a low ^{10}Be content, whereas AL25 is a graywacke clast with a high ^{10}Be content.

Increased ^{10}Be Signal as a Result of Contamination by ^{10}Be Derived from an Impactor

The cosmic rays flux is much higher in space than on the surface of the Earth and because of that the concentrations of the ^{10}Be within meteorites tend to be higher than those measured within terrestrial materials (e.g., Jull 2006; Welten et al. 2008; Dunai 2010). In theory, even small amounts of meteoric material mixed with Bosumtwi target rocks could significantly change ^{10}Be concentrations observed in the suevite. We have

calculated the possible extent of the ^{10}Be enrichment from the meteoritic material. We used the following assumptions: the impactor has ordinary-chondritic composition (Koeberl et al. 2007c), 800 m in diameter and is moving with 22 km s^{-1} (Artemieva et al. 2004), the volume of the transient cavity calculated according to Schmidt and Housen (1987), and most of the ^{10}Be present in the large asteroid is within the first 300 g cm^{-2} with the average contents within this layer corresponding to 10 dpm kg^{-1} (e.g., Jull 2006). The calculation shows that if we assume good mixing between impactor and target material from within the transient cavity, the material should be enriched up to about 0.1×10^6 at/g. This value is below the detection limit of the current study, and is about three times lower than values measured for samples AL25 and AL41.

Of course it is not impossible that mixing between impactor and target rocks was not homogeneous and some breccias were more highly enriched in ^{10}Be then others. However, such an explanation does not correspond to the results obtained in our study. Both samples with detectable ^{10}Be signal are clasts of graywacke, with no petrologic indications of any extraterrestrial material incorporation as visible in the thin section. In addition, to limit the possibility of this type of contamination, only internal parts of all studied clasts were selected for the ^{10}Be measurement. An explanation of the obtained data by admixture of the ^{10}Be derived from the impactor seems, therefore, very unlikely. This agrees with absence (or very low amount) of meteoritic components in the impact breccia (e.g., McDonald et al. 2007).

Increased ^{10}Be Signal as a Result of the Muonic Production at Great Depth

More than 98% of the ^{10}Be in the surface layer is produced from interactions of the target material with neutrons (e.g., Brown et al. 1995; Braucher et al. 2003, 2013). At depths greater than 1000 g cm^{-2}, the muonic component of ^{10}Be production is dominant (Braucher et al. 2013). However, the results obtained in this study cannot be explained by the postimpact muonic production within the crater (but probably this mechanism played some role in producing ^{10}Be in the preimpact target rocks from which clasts with an elevated content were derived) because of three main reasons. First, the production rate by muonic component is very low—on the order of 0.028 ± 0.004 at/g*a scaled to the sea level surface (Braucher et al. 2013). This leads to a very simplified (not corrected for altitude and latitude) calculation of the muonic contribution at a 1 Ma old surface of about 28,000 ^{10}Be at/g. This is only about 10% of the value measured by us within samples AL25 and AL41. Second, all analyzed samples come from below the surface. ^{10}Be production at the sample depth within the drill core is significantly lower due to the shielding effect of the lake water (layer of 69 m) overlaying lake sediments (thickness of 261 m) and impactites (25 and 53 m thick, respectively) (Koeberl et al. 2007a). And even if the attenuation length for muons (up to 5000 g cm^{-2}; Braucher et al. 2013) is significantly higher than for neutron production, all our samples are very well shielded from the muonic ^{10}Be production (being well below the detection limit of this study). Third, if the ^{10}Be within our samples would be derived from muonic postimpact production, then the depth profile should be uniformly enriched, with the highest ^{10}Be values at the top of the profile. In our study, we have observed the opposite—the enrichment in ^{10}Be is variable and not correlated with the depth in the drill core. In conclusion, muonic production of ^{10}Be cannot explain observed data.

Increased ^{10}Be Signal as a Result of the Surface Exposure of the Clasts Prior to the Bosumtwi Crater Formation

After excluding alternative hypotheses, the most probable explanation of the observed elevated ^{10}Be signal in samples AL25 and AL41 seems to be their near-surface exposure prior to the Bosumtwi crater formation. However, the exact determination of the clast's depth of origin within the preimpact target material is not possible because of the following reasons. First, the total ^{10}Be contents generally decrease with depth within weathering profile, although some profiles can have a more complex shape (Graly et al. 2010). No data about ^{10}Be in deep profiles within soils in the proximity of the Bosumtwi crater are available; the only data are from shallow profiles less than one meter deep (Serefiddin et al. 2007), even if soil profiles can be as thick as 8 m and the underlying saprolite being more than 30 m thick (Boamah and Koeberl 2003). Potentially comparable, several meters deep profiles are available from the Ivory Coast and Mali (Barg et al. 1997). However, because all of the available data are based on the studies of the fine fraction of the soils, not clasts within them, the data are not easily comparable. It is reasonable to expect that the average ^{10}Be contents of the clasts within soil profiles (or saprolite) are lower than that within the finer fraction of the soil (Graly et al. 2010), but it is very hard to properly assess the expected ^{10}Be concentration within a clast.

As ^{10}Be is a radionuclide with a half-life of 1.386 ± 0.016 Ma (Chmeleff et al. 2010) and the Bosumtwi impact crater is 1.07 million years old (Koeberl et al. 1997), it was necessary to recalculate concentrations of

^{10}Be in the AL25 and AL41 samples for the time when the impact happened. The decay-corrected values are $(0.37 \pm 0.23) \times 10^6$ at/g for sample AL41b and $(0.48 \pm 0.28) \times 10^6$ at/g for sample AL25. For comparison, the ^{10}Be content of the shallow soil cores (0–0.9 m) was measured to be from $133 \pm 12 \times 10^6$ at/g at depth 0.5 m up to $437 \pm 23 \times 10^6$ at/g (Serefiddin et al. 2007). This value is much higher because it comes from much shallower depths and also as it has a much higher surface area for meteoric ^{10}Be to adhere to. Geographically closest deeper ^{10}Be profiles were measured within analogous tropical oxic soils of the Ivory Coast (Barg et al. 1997). The ^{10}Be contents at the depths of 1.8 m, 4 m, and 10 m were 150×10^6 at/g, 35×10^6 at/g, and 40×10^6 at/g, respectively. Again, those values were measured on soil-saprolite samples where total surface area is much higher than within the uniform clast. No other data on ^{10}Be (in situ and meteoric) from comparable geographical locations are available. Based on available information and assuming the relatively uniformly decreasing ^{10}Be profile within the Bosumtwi crater target rocks sequence, and assuming that values within average soil and clasts are similar, we can estimate that both samples probably come from similar range of depths within the target rocks. The guesstimate of depth of clasts AL25 and AL41 origin is very tentative, but most probably they come from somewhere between 10 and 30 m depth.

Inferences for Crater-Forming Mechanism

The degree of mixing of the target material during the impact cratering process has been studied only to a very limited extent. Within the Kärdla structure, a 4 km diameter, well-preserved 455 Ma crater formed within a shallow sea, the impactites are very clearly stratified (Puura et al. 2004). The limestone that was forming a topmost 25 m layer of sedimentary target rocks is present only within the top 40 m of impactite strata that was interpreted to be a sedimentary slump and resurge breccia (Puura et al. 2004). This suggests that mixing of the target material during the impact cratering process was limited by the interaction with the layer of water (Melosh 1989; Ormö and Lindstrom 2000; Ormö et al. 2010; Wünnemann et al. 2010).

The mechanisms leading to the concentration of the target surface layer in resurge breccia of submarine craters are not present in subaerial craters. The research of the small subaerial impact crater Tswaing (1.13 km in diameter, 0.22 Ma old crater in South Africa) showed that about 2% of the thin layer of diatomite, siltstone, and shale, originally forming a few meters thick layer (<20 m) on the surface of the target rocks, was incorporated into the "sandy" impact breccia present in this crater (Reimold et al. 1992). However, no information about the arrangement of the surface component within the drill core was provided, and because the drill core is no longer available, it is impossible to perform a more detailed study on this topic.

The results of our study suggest that in the case of the Bosumtwi crater, it is possible to identify clasts that were located relatively close to the surface prior to the impact and that they are not concentrated within top layer of impactites (they were found at different depths within the breccia). Samples AL25 and AL41 are characterized by a different ^{10}Be concentration than the other samples that were located close to them in the drill core. This is consistent with the relatively efficient mixing of the material during the impact cratering process; otherwise, we should expect to find other clasts enriched in ^{10}Be close by. Two samples, AL22 (suevite) and AL45 (granite), with ^{10}Be concentration different from the process blank on 2σ level, are located close to each other at depths of 377.0 and 378.6 m (and close to the AL41). If we assume that those samples truly include some ^{10}Be, then they could represent a poorly mixed layer of clast-rich suevite formed from material that was originally located close to preimpact target surface or a material slumped during the modification stage.

In the case of the Bosumtwi crater, if the entire surface layer (about 25 m thickness) was perfectly mixed in the transient crater cavity, it would form up to approximately 5% of the crater-fill material. In reality, this percentage is probably lower due to: (1) the tendency of the surface layer to be removed from the crater in the form of ejecta, including tektites (Pal et al. 1982; Artemieva 2000; Serefiddin et al. 2007); (2) being vaporized/melted during the impact process (Melosh 1989), thus decreasing the potential number of clasts that can survive impact and be incorporated within crater-filling breccias; and (3) the surface layer being more weathered and less resistant to mechanical stress. Of course if mixing was not close to perfect, there can be some layers within the drill core characterized by a much higher percentage of the surface material. The particles with ^{10}Be contents suggestive of their origin close to the surface were detected on two different depths within the drill core (AL41: 355.5 m and AL25: 383.4 m). This shows that the surface component within the Bosumtwi crater drill core was not concentrated within the top layer of the fallback breccia, as was the case at Kärdla (Puura et al. 2004).

Both of the clasts (AL25 and AL41) with elevated ^{10}Be contents are graywackes. This is consistent with the predictions based on the characteristics of the geology in the proximity of Bosumtwi crater (e.g., Koeberl and Reimold 2005; Karikari et al. 2007; Losiak

et al. 2013). Most of the rocks present at the surface are meta-graywacke (Koeberl and Reimold 2005), with only approximately 2% addition of a granitoid component (Reimold et al. 1998).

Implications for Formation of the Crater-Related Pitted Materials on Mars

Our study has some implications for research on Martian impact craters. Mouginis-Mark et al. (2003) identified a new type of an impact ejecta and crater-fill facies on Mars: a thin layer of ejected materials densely covered with relatively small pits (approximately 10 m to 3 km in diameter) (Tornabene et al. 2012). Boyce et al. (2012) proposed a numerical model of pits formation by the explosive degassing of water from the water-bearing, impact melt-rich breccia. However, this model works only if the suevite is composed of very well-mixed target material (Boyce et al. 2012). Our research supports this model by demonstrating that material coming from different depths within the target rocks is well mixed within the topmost suevite layer.

CONCLUSIONS

We have conducted a study on the material from the drill cores from the Bosumtwi impact crater to determine the extent of mixing of target rocks during crater formation with respect to the crater-filling breccia. We have detected a ^{10}Be signal in 2 out of 29 samples. After excluding other possibilities that may explain the elevated ^{10}Be signal, we conclude that the elevated content of ^{10}Be within two graywacke clasts (AL25 and AL41), collected from the impactites from Bosumtwi impact drill core LB-07A, is most probably due to a preimpact origin of those clasts in a layer of the target rocks close to the surface (20–30 m).

The location of the samples with ^{10}Be concentrations suggestive of their surface origin within the drill core suggests efficient mixing of material forming in-crater breccia during the impact cratering process. This supports observations from the experimental and numerical modeling studies that in-crater breccia within submarine and subaerial craters form differently (e.g., Ormö et al. 2010).

The lack of a ^{10}Be signal within the rocks located very close to the boundary between lake-sediments and impactites suggests that infiltration of the meteoric water within the crater floor was very limited. The impactites were separated relatively efficiently from the surface water influence probably by the topmost fallback layer described by Koeberl et al. (2007b). A similar layer was probably present on the entire crater floor, apparently creating a barrier between lake and impactite deposits. Later on, this separation could have been increased by the thick layer of lake sediments being deposited. This may suggest that infiltration of meteoric water within a crater takes place not through the aerial pore-space infiltration, but rather through a localized system of fractures.

Acknowledgments—We acknowledge funding from the University of Vienna doctoral school IK-1045 and the Austrian Science Foundation grant P21821-N19. We are grateful to Ronald Conze for assistance during the sampling of the Bosumtwi cores in Potsdam core repository and to Peter Steier for performing one of the measurements and assistance with data reduction. We thank Matthew Huber for proofreading the manuscript. We thank two anonymous reviewers and editor Tim Jull for very helpful comments that significantly improved the manuscript.

Editorial Handling—Dr. A. J. Timothy Jull

REFERENCES

Artemieva N. A. 2000. Tektite origin in oblique impacts: Numerical modeling of the initial stage. In *Impacts in Precambrian shields*, edited by Plado J. and Pesonen L. J. Heidelberg-Berlin: Springer. pp. 257–276.

Artemieva N., Karp T., and Milkereit B. 2004. Investigating the Lake Bosumtwi impact structure. Insight from numerical modeling. *Geochemistry Geophysics Geosystems* 11:Q11016, doi:10.1029/2004GC000733.

Auer M. 2007. Applications of ^{26}Al in atmospheric research. Ph.D. thesis, University of Vienna, Vienna, Austria.

Auer M., Kutschera W., Priller A., Wagenbach D., Wallner A., and Wild E. M. 2007. Measurement of ^{26}Al for atmospheric and climate research and the potential of ^{26}Al/^{10}Be ratios. *Nuclear Instruments and Methods in Physics Research Section B* 259:595–599.

Barg E., Lal D., Pavich M. J., Caffee M. W., and Southon J. R. 1997. Beryllium geochemistry in soils; evaluation of ^{10}Be/^{9}Be ratios in authigenic minerals as a basis for age models. *Chemical Geology* 140:237–258.

Boamah D. and Koeberl C. 2003. Geology and geochemistry of shallow drill cores from the Bosumtwi impact structure, Ghana. *Meteoritics & Planetary Science* 38:1137–1159.

Boyce J. M., Wilson L., Mouginis-Mark P. J., Hamilton C. W., and Tornabene L. L. 2012. Origin of small pits in martian impact craters. *Icarus* 221:262–275.

Braucher R., Brown E. T., Bourles D. L., and Colin F. 2003. In situ produced ^{10}Be measurements at great depths: Implications for production rates by fast muons. *Earth and Planetary Science Letters* 211:251–258.

Braucher R., Bourles D., Merchel S., Romani J. V., Fernandez-Mosquera D., Marti K., Leanni L., Chauvet F., Arnold M., Aumaitre G., and Keddadouche K. 2013. Determination of muon attenuation lengths in depth profiles from in situ produced cosmogenic nuclides. *Nuclear Instruments and Methods in Physics Research Section B* 294:484–490.

Brown E. T., Edmond J. M., Raisbeck G. M., Bourlès D., Yiou F., and Measures C. 1992. Beryllium isotope geochemistry in tropical river basins. *Geochimica et Cosmochimica Acta* 56:1607–1624.

Brown E. T., Bourles D. L., Colin F., Raisbeck G. M., Yiou F., and Desgarceaux S. 1995. Evidence for muon-introduced production of ^{10}Be in near-surface rocks from the Congo. *Geophysical Research Letters* 22:703–706.

Chmeleff J., von Blanckenburg F., Kossert K., and Jakob D. 2010. Determination of the ^{10}Be half-life by multicollector ICP-MS and liquid scintillation *counting*. *Nuclear Instruments and Methods in Physics Research Section B* 268:192–199.

Coney L., Gibson R. L., Reimold W. U., and Koeberl C. 2007. Lithostratigraphic and petrographic analysis of ICDP drill core LB-07A, Bosumtwi impact structure, Ghana. *Meteoritics & Planetary Science* 42:569–589.

Dunai T. J. 2010. *Cosmogenic nuclides, principles, concepts and applications in the earth surface sciences*. New York: Cambridge University Press. 187 p.

Engelhardt W. von, Berthold C., Wenzel T., and Dehner T. 2005. Chemistry, small-scale inhomogeneity, and formation of moldavites as condensates from sands vaporized by the Ries impact. *Geochimica et Cosmochimica Acta* 69:5611–5626.

Ferrière L., Koeberl C., and Reimold W. U. 2007a. Drill core LB-08A, Bosumtwi impact structure, Ghana: Petrographic and shock metamorphic studies of material from the central uplift. *Meteoritics & Planetary Science* 42:611–633.

Ferrière L., Koeberl C., and Reimold W. U. 2007b. Drill core LB-08A, Bosumtwi impact structure, Ghana: Geochemistry of fallback breccia and basement samples from the central uplift. *Meteoritics & Planetary Science* 42:689–708.

Ferrière L., Koeberl C., Ivanov B., and Reimold W. U. 2008. Shock metamorphism of Bosumtwi impact crater rocks, shock attenuation, and uplift formation. *Science* 322:1678–1681.

Ferrière L., Koeberl C., Reimold W. U., Hecht L., and Bartosova K. 2009. The origin of "toasted" quartz in impactites revisited (abstract #1751). 40th Lunar and Planetary Science Conference. CD-ROM.

Ferrière L., Koeberl C., Brandstätter F., and Mader D. 2010. Geochemistry of basement rocks and impact breccias from the central uplift of the Bosumtwi crater, Ghana—Comparison of proximal and distal impactites. In *Large meteorite impacts and planetary evolution IV*, edited by Gibson R. L. and Reimold W. U. GSA Special Paper 465. Boulder, Colorado: Geological Society of America. pp. 443–469.

Feybesse J., Billa M., Guerrot C., Duguey E., Lescuyer J., Milesi J., and Bouchot V. 2006. The paleoproterozoic Ghanaian province: Geodynamic model and ore controls, including regional stress modeling. *Precambrian Research* 149:149–196.

Franklin C. 2007. *Statistics the art and science of learning from data*. Upper Saddle River, New Jersey: Pearson Prentice Hall. 693 p.

Gosse J. C. and Phillips F. M. 2001. Terrestrial in situ cosmogenic nuclides: Theory and application. *Quaternary Science Reviews* 20:1475–1560.

Graham I., Ditchburn R., and Barry B. 2003. Atmospheric deposition of ^{7}Be and ^{10}Be in New Zealand rain (1996–98). *Geochimica et Cosmochimica Acta* 67:361–373.

Graly J. A., Bierman P. R., Reusser L. J., and Pavich M. J. 2010. Meteoric ^{10}Be in soil profiles—A global meta-analysis. *Geochimica et Cosmochimica Acta* 74:6814–6829.

Heikkilä U., Beer J., and Alfimov V. 2008. Beryllium-10 and Beryllium-7 in precipitation in Dübendorf (440 m) and at Jungfraujoch (3580 m), Switzerland (1998-2005). *Journal of Geophysical Research* 113:D11104. doi:10.1029/2007JD 009160.

Hofmann H. J., Beer J., Bonani G., von Gunten H. R., Raman S., Suter M., Walker R. L., Walfli W., and Zimmermann D. 1987. ^{10}Be: Half life and AMS-standards. *Nuclear Instruments and Methods in Physics Research Section B* 29:32–36.

Jones W. B. 1985. Chemical analyses of Bosumtwi crater target rocks compared with the Ivory Coast tektites. *Geochimica et Cosmochimica Acta* 48:2569–2576.

Jones W. B., Bacon M., and Hastings D. A. 1981. The Lake Bosumtwi impact crater, Ghana. *Geological Society of America Bulletin* 92:342–349.

Jull A. J. T. 2006. Terrestrial ages of meteorites. In *Meteorites and the early solar system*, edited by Lauretta D. S. and McSween H. Y. Jr. Tucson, Arizona: The University of Arizona Press. pp. 889–905.

Karikari F., Ferriere L., Koeberl C., Reimold W. U., and Mader D. 2007. Petrography, geochemistry, and alteration of country rocks from the Bosumtwi impact structure, Ghana. *Meteoritics & Planetary Science* 42:513–540.

Koeberl C. 1986. Geochemistry of tektites and impact glasses. *Annual Review of Earth and Planetary Sciences* 14:323–350.

Koeberl C. 1994. Tektite origin by hypervelocity asteroidal or cometary impact: Target rocks, source craters, and mechanisms. In *Large meteorite impacts and planetary evolution*, edited by Dressler B. O., Grieve R. A. F., and Sharpton V. L. GSA Special Paper 293. Boulder, Colorado: Geological Society of America. pp. 133–151.

Koeberl C. and Reimold W. U. 2005. Bosumtwi impact crater, Ghana (West Africa): An updated and revised geological map, with explanations. *Jahrbuch der Geologischen Bundesanstalt, Wien (Yearbook of the Austrian Geological Survey)* 145:31–70 (+1 map, 1:50,000).

Koeberl C., Bottomley R., Glass B., and Storzer D. 1997. Geochemistry and age of Ivory Coast tektites and microtektites. *Geochimica et Cosmochimica Acta* 61:1745–1772.

Koeberl C., Milkereit B., Overpeck J. T., Scholz C. A., Amoako P. Y. O., Boamah D., Danuor S. K., Karp T., Kueck J., Hecky R. E., King J., and Peck J. A. 2007a. An international and multidisciplinary drilling project into a young complex impact structure: The 2004 ICDP Bosumtwi impact crater, Ghana, drilling project—An overview. *Meteoritics & Planetary Science* 42:483–511.

Koeberl C., Brandstaetter F., Glass B. P., Hecht L., Mader D., and Reimold W. U. 2007b. Uppermost impact fallback layer in the Bosumtwi crater (Ghana): Mineralogy, geochemistry, and comparison with Ivory Coast tektites. *Meteoritics & Planetary Science* 42:709–729.

Koeberl C., Shukolyukov A., and Lugmair G. W. 2007c. Chromium isotopic studies of terrestrial impact craters: Identification of meteoritic components at Bosumtwi, Clearwater East, Lappajärvi, and Rochechouart. *Earth and Planetary Science Letters* 256:534–546.

Korkisch J. 1989. *Handbook of ion exchange resins*. Boca Raton, Florida: CRC Press. 352 p.

Korschinek G., Bergmaier A., Faestermann T., Gerstmann U., Knie K., Rugel G., Wallner A., Dillmann I., Dollinger G., von Gostomski C. L., Kossert K., Maiti M., Poutivtsev

M., and Remmert A. 2010. A new value for the half-life of ^{10}Be by heavy-ion elastic recoil detection and liquid scintillation counting. *Nuclear Instruments and Methods in Physics Research Section B* 268:187–191.

Kutschera W., Collon P., Friedmann H., Golser R., Hille P., Priller A., Rom W., Steier P., Tagesen S., Wallner A., Wild E., and Winkler G. 1997. VERA: A new AMS facility in Vienna. *Nuclear Instruments and Methods in Physics Research Section B* 123:47–50.

Leube A., Hirdes W., Maur R., and Kesse G. O. 1990. The early Proterozoic Birimian Supergroup of Ghana and some aspects of its associated gold mineralization. *Precambrian Research* 46:139–165.

Losiak A., Schulz T., Buchwaldt R., and Koeberl C. 2013. Petrology, major and trace element geochemistry, geochronology, and isotopic composition of granitic intrusions from the vicinity of the Bosumtwi impact crater, Ghana. *Lithos* 177:297–313.

Ma P., Aggrey K. A., Onzola C. T., Chnabel C. S., Icola P. D. E. N., Erzog G. F. H., Asson J. T. W., and Lass B. P. G. 2004. Beryllium-10 in Australasian tektites: Constraints on the location of the source crater. *Geochimica et Cosmochimica Acta* 68:3883–3896.

Martschini M. 2008. ^{10}Be-^{10}B isobar separation with a degrader foil: Implementation and testing of an optimized ion-optical setup for AMS of ^{10}Be. Diploma thesis, University of Vienna, Vienna, Austria.

McDonald I., Peucker-Ehrenbrink B., Coney L., Ferriere L., Reimold W. U., and Koeberl C. 2007. Search for a meteoritic component in drill cores from the Bosumtwi impact structure Ghana: Platinum-group element contents and osmium isotopic characteristics. *Meteoritics and Planetary Science* 42:743–753.

Melosh H. J. 1989. *Impact cratering*. New York: Oxford University Press, Clarendon Press.

Merchel S. and Herpers U. 1999. An update on radiochemical separation techniques for the determination of long-lived radionuclides via accelerator mass spectrometry. *Radiochimica Acta* 84:215–219.

Michlmayr L. 2007. Isobar separation with post-stripping for the measurement of cosmogenic ^{10}Be at VERA. Diploma thesis, University Vienna, Vienna, Austria. http://othes.univie.ac.at/5278/1/Diplomarbeit-Michlmayr.lin.pdf

Moon P. A. and Mason D. 1967. The geology of 1/4° field sheets nos. 129 and 131, Bompata S.W. and N.W. *Ghana Geological Survey Bulletin* 31:1–51.

Mouginis-Mark P., Boyce J. M., Hamilton V. E., and Anderson F. S. 2003. A very young, large impact crater on Mars (abstract #3004). Sixth International Conference on Mars July 20–25 2003, Pasadena, CA.

Nishiizumi K., Imamura M., Caffee M. W., Southon J. R., Finkel R. C., and McAninch J. 2007. Absolute calibration of ^{10}Be AMS standards. *Nuclear Instruments and Methods in Physics Research Section B* 258:403–413.

Ormö J. and Lindstrom M. 2000. When a cosmic impact strikes the sea bed. *Geological Magazine* 137:67–80.

Ormö J., Lepinette A., Sturkell E., Lindstrom M., Housen K. R., and Holsapple K. A. 2010. Water resurge at marine-target impact craters analyzed with a combination of low-velocity impact experiments and numerical simulations. In *Large meteorite impacts and planetary evolution IV*, edited by Gibson R. L. and Reimold W. U. GSA Special Paper 465. Boulder, Colorado: Geological Society of America. pp. 81–101.

Pal D. K., Tuniz C., Moniot R. K., Kruse T. H., and Herzog G. F. 1982. Beryllium-10 in Australasian tektites: Evidence for a sedimentary precursor. *Science* 218:787–789.

Pavich M. J., Brown L., Valette-Silver J. N., Klein J., and Middleton R. 1985. ^{10}Be analysis of a Quaternary weathering profile in the Virginia Piedmont. *Geology* 13:39–41.

Petersen M. T., Newsom H. E., Nelson M. J., and Moore D. M. 2007. Hydrothermal alteration in the Bosumtwi impact structure: Evidence from 2M1-muscovite, alteration veins, and fracture fillings. *Meteoritics & Planetary Science* 42:655–666.

Puura V., Huber H., Kirs J., Karki A., Suuroja K., Kirsimae K., Kivisilla J., Kleesment A., Konsa M., Preeden U., Suuroja S., and Koeberl C. 2004. Geology, petrography, shock petrography, and geochemistry of impactites and target rocks from the Kärdla crater, Estonia. *Meteoritics & Planetary Science* 39:425–451.

Reimold W. U., Koeberl C., Partridge T. C., and Kerr S. J. 1992. Pretoria Saltpan crater: Impact origin confirmed. *Geology* 20:1079–1082.

Reimold W. U., Brandt D., and Koeberl C. 1998. Detailed structural analysis of the rim of a large, complex impact crater: Bosumtwi crater, Ghana. *Geology* 26:543–546.

Schmidt R. M. and Housen K. R. 1987. Some recent advances in the scaling of impact and explosion cratering. *International Journal of Impact Engineering* 5:543–560.

Serefiddin F., Herzog G. F., and Koeberl C. 2007. Beryllium-10 concentrations of tektites from the Ivory Coast and from Central Europe: Evidence for near-surface residence of precursor materials. *Geochimica et Cosmochimica Acta* 71:1574–1582.

Shanahan T. M., Beck J. W., Overpeck J. T., McKay N. P., Pigati J. S., Peck J. A., Scholz C. A., Heil C. W. Jr., and King J. 2012. Late Quaternary sedimentological and climate changes at Lake Bosumtwi Ghana: New constraints from laminae analysis and radiocarbon age modeling. *Palaeogeography, Palaeoclimatology, Palaeoecology* 361–362:49–60.

Shen C. D., Beer J., Kubik P. W., Suter M., Borkovec M., and Liu T. S. 2004. Grain size distribution, ^{10}Be content and magnetic susceptibility of micrometer-nanometer loess materials. *Nuclear Instruments and Methods in Physics Research Section B* 223–224:613–617.

Son T. H. and Koeberl C. 2007. Chemical variation in Lonar impact glasses and impactites. *GFF* 129:161–176.

Steier P., Golser R., Kutschera W., Priller A., Vockenhuber C., and Winkle S. 2004. VERA, an AMS facility for "all" isotopes. *Nuclear Instruments and Methods in Physics Research Section B* 223–224:67–71.

Tornabene L. L., Osinski G. R., McEwen A. S., Boyce J. M., Bray V. J., Caudill C. M., Grant J. A., Hamilton C. W., Matttson S., and Mouginis-Mark P. J. 2012. Widespread crater-related pitted materials on Mars: Further evidence for the role of target volatiles during the impact process. *Icarus* 220:348–368.

Turner B. F., Gardner L. R., and Sharp W. E. 1996. The hydrology of Lake Bosumtwi, a climate sensitive lake in Ghana, West Africa. *Journal of Hydrology* 183:243–261.

Wasson J. T. 2003. Large aerial bursts: An important class of terrestrial accretionary events. *Astrobiology* 3:163–179.

Welten K. C., Folco L., Nishiizumi K., Caffee M. W., Grimberg A., Meier M. M. M., and Kober F. 2008. Meteoritic and bedrock constraints on the glacial history

of Frontier Mountain in northern Victoria Land, Antarctica. *Earth and Planetary Science Letters* 270:308–315.

Willenbring J. K. and von Blanckenburg F. 2010. Meteoric cosmogenic Beryllium-10 adsorbed to river sediment and soil: Applications for Earth-surface dynamics. *Earth-Science Reviews* 98:105–122.

Wünnemann K., Collins G. S., and Weiss R. 2010. Impact of a cosmic body into Earth's ocean and the generation of large tsunami waves: Insight from numerical modeling. *Reviews of Geophysics* 48:RG4006, doi:10.1029/2009RG000308.

You C.-F., Lee T., and Li Y.-H. 1989. The partition of Be between soil and water. *Chemical Geology* 77:105–118.